

# Investigation of Pumping Action of Bubble Pump of Diffusion-Absorption Cycles

Ali Benhmidene<sup>1</sup>

<sup>1</sup> The National School of Engineering of Gabes, Tunisia

Received: 11 December 2016 Accepted: 1 January 2017 Published: 15 January 2017

---

## Abstract

In the diffusion absorption machines, there is not a mechanical pump for circulating the working fluid. This role is provided by the thermal bubble pump. The efficiency of diffusion absorption cycles is related of the pumping action of the bubble pump. The aim of the present numerical study is to investigate the influence of tube diameter, heat input, tube length and mass flow rate on the pumping action of solar bubble pump. A onedimensional two-fluid model was developed under constant heat flux for predict the behaviour of pumping ratio under permanent regime. At a fixed bubble pump tube length of 1m, and ammonia mass fraction of 0.4 and pressure 18 bar at the inlet, numerical results show that, the pumping ration is mostly influences by heat input. Its maximum is directly related by the mass flow rate and tube diameter.

---

*Index terms*— bubble pump, pumping ratio, numerical study, operating conditions.

## 1 Introduction

onventional vapour compression and absorption refrigeration systems are based on cycles in which the refrigerant is circulated by a compressor or a mechanical pump, correspondingly. Compressor or pump operation requires a mechanical input, which adds significantly to the noise level and cost of the cooling system and reduces its reliability and portability [1].

A pumpless diffusion absorption refrigeration cycle is of great importance in silent refrigeration applications because it does not use a mechanical pump. The circulation of the fluid in the diffusion absorption cycle is ensured by a bubble pump under the effect of thermal energy [2]. Indeed the pump a bubble pump is a fluid pump that operates on thermal energy to pump the liquid from the lower level to the upper level. When heat is applied to the pump tube, the rich solution turns into two phases, liquid and vapour; this creates a two-phase flow. Dynamiting the gas creates a pump-like effect that pushes the boiling water to a higher elevation.

There are several parameters of the bubble pump which can be adjusted to optimize its pumping action. These parameters include: the diameter of the lift tube [1,3,4], the heat input [5,6], working fluid [7] and the level of pressure. For tube lift diameter range, since a bubble pump operates most efficiently in the slug flow regime [8]. The maximum diameter tube in which slug flow occurs is given by the Chisholm equation [9]. When the maximum lift-tube diameter is exceeded, the flow pattern changes from slug flow to an intermittent churn type flow [10]. After a certain pumping height is exceeded, the pumping action stopped. But under effect heat fluctuation, such as for heating solar, it's difficult of bubble pump to stay in this regime. In this topic While [10] shows that a smaller than optimal diameter lift tube will experience churn flow and a much higher than optimal diameter tube will produce bubbly flow.

Pfaff et al. [11] studied the bubble pump operating with Li-Bre-H<sub>2</sub>O. They found that for a tube diameter of 10 mm, the pumping action accrued at 30W; however the heat input is around 40W for a diamond of 14mm. And the frequency of the pumping action increases as the heat input to the bubble pump increases or the tube diameter decreases. Using a water-amminiac system, the authors showed that the diameter which maximizes the

44 efficiency of the bubble pump is between 4 mm and 26 mm for a liquid pumping rate of between 0.0025 kg /  
 45 s and 0, 02 kg / s. However, efficiency decreases rapidly when diameters below optimal values are used; they  
 46 recommend, therefore, that the diameter should be slightly higher than the optimum value found.

47 Another widely studied factor is the variable heat input to the bubble pump. In this subject, two parameters  
 48 were studied as a function of the heat input: liquid and vapour mass flow which characterize the efficiency of the  
 49 bubble pump [12][13][14][15][16]. These studies showed that the mass flow rate of the steam increased linearly  
 50 with the heat input, while the mass flow rate of the pumped liquid increased before it reached a maximum value,  
 51 after which it decreased with the increase in heat input. Thus, the optimum heat input is which corresponding to  
 52 the amount of maximum pumped liquid. The optimum heat input range is function of working fluid concentration  
 53 [17], submersion ratio [16,18] and bubble pump characteristics [15,19].

54 Faisal [20] studied the performance of LiBr-H<sub>2</sub>O pumpless absorption refrigeration system. A simulated test  
 55 rig of the thermal bubble pump was fabricated using water as a test fluid. For a tube length of 1.5m, author  
 56 tested 3 diameters 6.5, 10 and 14mm. He found that at a temperature of between 102 ° C and a tube diameter  
 57 of 10 C Year 2017 Global Journal of Researches in Engineering ( ) Volume XVII Issue IV Version I A mm, the  
 58 pumping capacity reached its maximum of 0.0295kg / s and 0.043kg / s respectively for the submersion ratios  
 59 0.5 and 0.7. In addition the pumping capacity decreases for large drop in heat input. The same tendency of the  
 60 variation for the pumping ratio with the heat yielded for the other tube diameters. The experimental results  
 61 show that the slug regime is dominant for the maximum pumping ratio of the bubble pump.

62 Numerical study conducted by Benhmidene et al. [12] were defined the minimum heat input required of  
 63 pumping action. They have been correlated in function of tube diameter. In the same work authors had  
 64 correlated the optimum heat input to require a maximum of amount of pumped liquid. The optimum heat  
 65 input is correlated in function of tube diameter and mass flow rate. As results of the same numerical modeling,  
 66 Benhmidene et al. [21] had justified the relation between pumping action and flow regime transition by studied  
 67 the variation of liquid velocity as function of vapor velocity. That cans allowed defining the maps flow regime as  
 68 function of heat input.

69 The aim of present work is to study the influence of operating conditions such as heat input, tube diameter  
 70 and mass flow rate on the pumping action. A numerical study based on two-fluid model was carried out to  
 71 achieve our goals. The bubble pump subject of the present study was a vertical uniformly heated tube with an  
 72 ammonia-water mixture (40% ammonia of ammonia).

## 73 2 II.

### 74 3 Mathematical Model

75 In the present study ammonia water solution is used as a working fluid. The main components of an absorption-  
 76 diffusion refrigeration cycle and flow configurations in the bubble pump are showing in Figure ??.

### 77 4 Fig. 1: Absorption diffusion machine and their compounds

78 The pumping ratio is defined as the ratio of mass flow of the pumped liquid and the vapour. To study the  
 79 pumping action, requires the knowledge of mass pumped liquid and flow. Heat applied to the bubble pump tube  
 80 causes a two-phase region. In the two-phase region, the general conservation equations of mass, momentum and  
 81 energy were formulated by Ishii and Mishima [22]. For the steady state with negligible kinetic and potential  
 82 energy, the conservation equations are reduced to the following five equations: Phase mass equations ( ) G G G  
 83  $d u dz = \hat{I}$  (1) ( ) 1 L L L d u dz =  $\hat{I}$  (2)

84 ? Phase momentum equations ( ) 2 G G G WL GL GI d dP u g F F F dz dz + + = ? ? ? (3) ( ) ( )  
 85 ( ) 2 1 1 1 L L L WL LG LI d dP u g F F F dz dz + + = ? + ? ? (4)

86 ? Mixture energy equation ( ) 1 w h L L L G G q P d u H u H dz A ? ? ? ? ? + = ? ? (5)

87 Closure relation and description of method resolution is detailed in [23]. Resolving of two-fluid model equation  
 88 allowed to determine void fraction, liquid and vapour mass flow, pressure and enthalpy of liquid.

89 To validate the two-fluid model results a comparison of the calculated values for void fraction versus vapour  
 90 quality using this model was compared with those obtained from three other models [24,25].

91 A good agreement between these results indicates that the two-fluid model is suitable for the prediction of  
 92 refrigerant two-phase flow in bubble pumps [23].

## 93 5 III.

### 94 6 Results and Discussion

95 Several operating parameters can influence the pumping action of the bubble pump. The studies are concentrated  
 96 on the pumping ratio as the magnitude characterizing this pumping action. Studies carried out by Benhmidene  
 97 et al. [17] are showing a weak influence of ammonia mass fraction on the pumping ratio. The same result was  
 98 obtained for the influence of the pressure at the inlet.

99 In the present study, we focus on the effect of the tube diameter and the heat flow on the pumping ratio. The  
 100 bubble pump tube length is fixed at 1m, pressure at the inlet is of 18bar and mass fraction of ammonia in strong

---

101 solution is 40%. The range of heat flux is chosen according to the solar intensity at the zone of Gabès in Tunisia  
102 where it is between 150 and 800W/m<sup>2</sup> [26].

103 Since the pumping action is optimal for the slug regime, we have used the Chisholm relation (Eq.6) [9] which  
104 fixes the upper tube diameter to have a slug regime.?? ? ? ?? ?? δ ??”δ ??” ?δ ??”.?1? ?? δ ??”δ ??” ?? δ ??”δ ??”  
105 ? ? 1/2(6)

106 Therefore, the behaviour of the pumping ratio is investigated for the tube diameters from 2mm to 14mm by  
107 increment of 2mm. In this diameter range, heat flux received by the tube of bubble pump without taking into  
108 account the losses will be taken between 5 and 50 kW/m<sup>2</sup>.

109 To define the working mass flow rate in this study, we follow the evolution of the pumping ratio as a function  
110 of mass flow rate this for a heat flux of 20kW/m<sup>2</sup>. According to Fig. ??, the pumping ratio increases if the mass  
111 flow rate increased, this is an expected behaviour since the liquid flow rate increases with this parameter too.  
112 However, it should be noted that the variation decreases with tube diameter. A small variation in the pumping  
113 ratio between the diameters 10, 12 and 14 mm can be observed.

114 Regarding those results, the mass flow rate choice is 50kg/m<sup>2</sup>.s because it’s the middle.

## 115 7 Fig.2: Pumping ratio vs mass flow rate

116 The pumping ratio is also studied in function of tube height. These variations are studied for tube diameter  
117 from 2 to 12mm. For a constant mass flow rate of 50kg/m<sup>2</sup>.s, Figure ?? 3 (a), (b), (c) shows the variation of the  
118 pumping ratio along tube respectively for 5, 20 and 50 kW/m<sup>2</sup>. These figures show a similar general behaviour  
119 for the different tube diameters and for the three heat flux, i.e., an increase, reaches a maximum and then a  
120 decrease, its value depends on heat flux.

121 The first result emerging from these curves is that the tube length where pumping ratio increase, decreases  
122 with the heat flux and increases with the tube diameter. For example, for the heat flux of 5kW / m<sup>2</sup>, except for  
123 the diameter of 2mm, the pumping ratio increases for the others diameters. By increasing the heat flux, zone  
124 of increasing will be between 10 and 40cm (Fig. 3.c). In addition, a higher pumping ratio is required at the  
125 outlet of the pump where the liquid is pumped to the separator. By examining the pumping ratio value at the  
126 outlet one notices its decrease as a function of heat flux as well as for descending tube diameter. Indeed for the  
127 diameter of 2mm, the ratio is about 0.2, and becomes null for the other heat fluxes, results allow us to limit the  
128 studies to the diameter of 4mm as lower value. It should be noted that the maximum pumping ratio increases  
129 along the tube to reach a maximum value of 0.4. The influence of heat flux will be studied in the next section.  
130 In this section, pumping ratio is studied in function of heat flux for different tube diameters. Figure ?? shows  
131 how the pumping ratio variation with the heat flux and tube diameter. It can be see that the pumping ratio  
132 increases with increasing the amount of the heat input until it reaches a maximum discharge point. Then any  
133 further increase in the supplied heat will cause the pumping ratio to become lower. The increase in pumping  
134 ratio for the low heat fluxes is due to the increase of the mass flow rate of pumping liquid with the increase of  
135 the steam flow rate. Indeed this zone will be characterized by a slug regime. The amount of vapour generated is  
136 capable of lifting the liquid. The heat flux corresponding to this zone varies 5 and 20kW / m<sup>2</sup>. The maximum  
137 value of the pump ratio is not too much influence by the diameter of the tube it is between 0.33 and 0.4, however  
138 the rate of increase of the maximum value decreases by increasing the tube diameter.

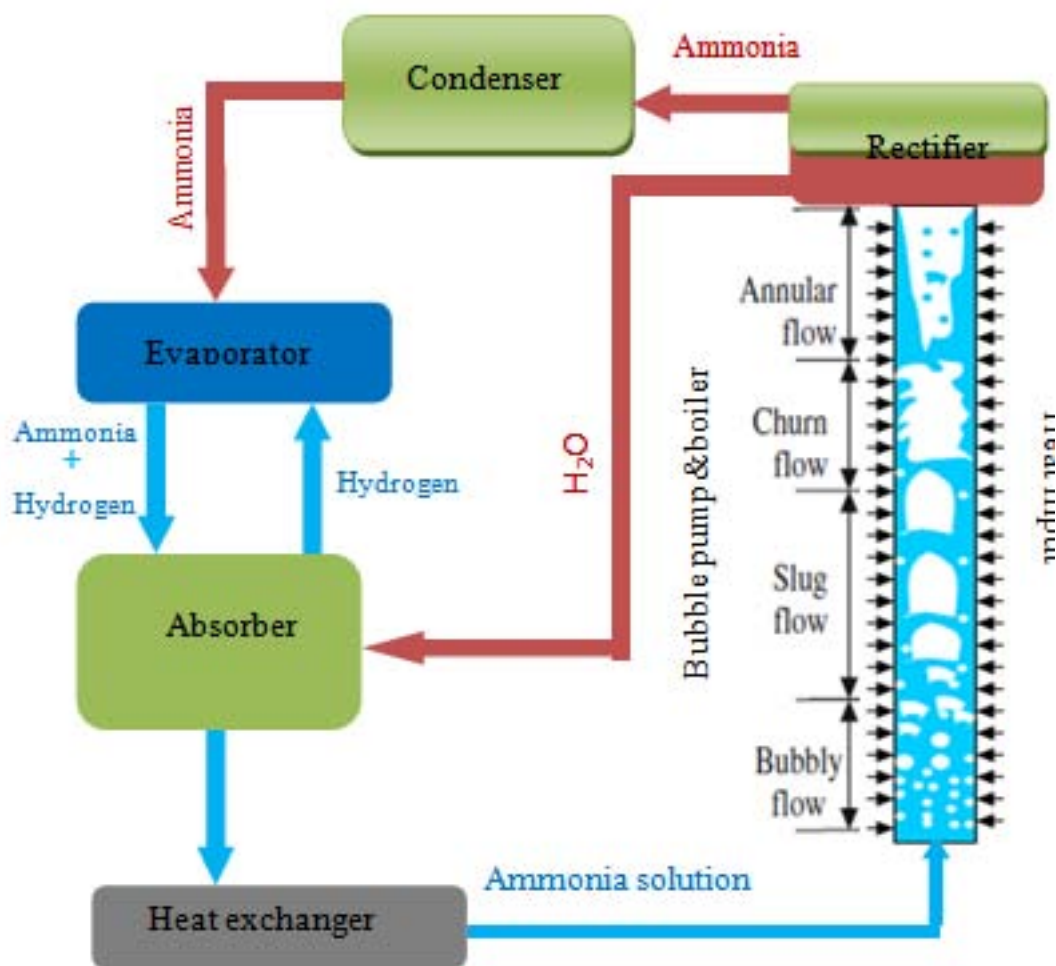
139 Under the effect of additional heat, the mass flow of the liquid pumping decreases. This leads to the apparition  
140 of an area for which the pumping ratio decreases. As an explanation of this behaviour is attributed, in greater  
141 proportion, to the increase of the frictional pressure drop (see Figure ??) due to the increase of the vapour mass  
142 flow rate and the variation of flow regime from slug to annular. In fact, in the annular flow pattern, the liquid  
143 dragged up mainly by the action of shear stress between high velocity vapour and the liquid and partially by  
144 the buoyancy action at which condition the slip ratio is too high. [27]. In this topic, a comprehensive study  
145 of flow regimes transition was carried out by Benhmidene et al. [21], in which authors show the reduction of  
146 the zone occupied by the slug regime vis-avis the churn and annular regimes when the heat flux increases. Our  
147 observations in this study coincide well with those of Jacob et al. [28], Shihab [29], Sathe [16]. When the received  
148 heat flux below an optimum value (corresponding to the maximum value of the pumping ratio), the buoyancy  
149 effect of the steam still has the ability to overcome the additional frictional pressure drop. This capacity appears  
150 in an additional increase of the pumped liquid to the maximum point. Bigger the tube diameter, bigger the  
151 optimum heat, where it increase from 7 to 25kW/m<sup>2</sup> where tube diameter increase from 4 to 12mm.

## 152 8 Conclusion

153 The pumping action of the bubble of diffusion absorption machines is numerically studied by using the two-fluid  
154 model. Equations balance of mass, momentum and energy of each phase are resolving with Matlab software.  
155 Numerical resolution allowed to define the pumping ratio, which is studied in function of tube length, mass  
156 flow rate, heat flux that for different tube diameter. The following conclusions have been drawn: -According its  
157 definition as a parameter characterised the pumping action, the pumping ration at the outlet of the bubble pump  
158 must be higher than zero, and thus the tube diameter minimum must be more than 4 mm. -The influence of  
159 tube diameter on pumping ratio by varying mass flow rate becomes lower for tube diameter higher than 10mm.  
160 -The pumping ratio is mostly function of heat flux. It increases for the range of heat flux where slug is the flow

## 8 CONCLUSION

161 regime. The maximum pumping ratio for each studied diameter tube is between 0.33 to 0.4. For the higher heat  
162 flux pumping ratio increase for all tube diameters under the influence of frictional pressure drop and flow regime  
163 transition from slug to annular. -The bubble pump optimum functioning are defined when the pumping ratio is  
164 maximal. The results shows, the value of heat flux corresponding to the optimal functioning are more influenced  
165 by tub diameter (3kW/m<sup>2</sup> for a 4mm of tube diameter and 5, 10, 13 and 17 kW/m respectively for 6, 8, 10 and  
166 12 mm of tube diameter). It increase with tube diameter, but it's weak influenced by varying of inlet pressure  
or ammonia fraction. <sup>1 2</sup>



3

Figure 1: Fig. 3 (

167

<sup>1</sup>© 2017 Global Journals Inc. (US)

<sup>2</sup>Investigation of Pumping Action of Bubble Pump of Diffusion-Absorption Cycles© 2017 Global Journals Inc. (US)

- 168 [Benhmidene et al. ()] ‘A Review of Bubble Pump Technologies’. A Benhmidene , B Chaouachi , S Gabsi . *J.*  
169 *Appl. Sci* 2010. 10 (16) p. .
- 170 [As Shihab ()] ‘An approach for modeling the performance of thermal bubble pump’. As Shihab . *The Iraqi*  
171 *Journal For Mechanical And Material Engineering* 2015. p. 15.
- 172 [Koyfman et al. ()] ‘An experimental investigation of bubble pump performance for diffusion absorption refriger-  
173 ation system with organic working fluids’. A Koyfman , M Jelinek , A Levy , I Borde . *App. Ther. Engineering*  
174 2003. 23 p. .
- 175 [White ()] *Bubbles pump design and performance*, S J White . 2001. Georgia Institute of Technology (M.Sc  
176 Thesis)
- 177 [Rouhani and Axelsson ()] ‘Calculation of volume void fraction in the subcooled and quality region’. Z Rouhani  
178 , E Axelsson . *Int J Heat Mass Transfer* 1970. 13 p. .
- 179 [Delano ()] *Design analysis of the Einstein refrigeration cycle*, A D Delano . 1998. Georgia Institute of Technology  
180 (Ph D Dissertation)
- 181 [Chaouachi and Gabsi ()] ‘Design and Simulation of an absorption diffusion solar refrigeration unit’. B Chaouachi  
182 , S Gabsi . *Am. J. Appl. Sci* 2007. 4 p. .
- 183 [Benhmidene et al. ()] ‘Effect of operating conditions on the performance of the bubble pump of absorption dif-  
184 fusion refrigeration cycles’. A Benhmidene , B Chaouachi , S Gabsi , M Bourouis . *Therm. Sc* 2011. 15 (3) p.  
185 .
- 186 [Zivi ()] ‘Estimation of steady state steam void fraction by means of principle of minimum entropy production’.  
187 S M Zivi . *Trans. ASME. J. Heat Transfer* 1964. 86 p. .
- 188 [Sathe ()] *Experimental and Theoretical Studies on a Bubble Pump for a Diffusion-Absorption Refrigeration*  
189 *System*, A Sathe . 2001. Indian Institute of Technology Madras and University of Stuttgart (Master’s thesis)
- 190 [Benhmidene et al. ()] ‘Experimental investigation on the flow behaviour in a bubble pump of diffusion absorption  
191 refrigeration systems, Case Stud’. A Benhmidene , Kh , B Hidouri , S Chaouachi , M Gabsi , Bourouis . *Therm*  
192 *Eng* 2016. 8.
- 193 [Ben Ezzine et al. ()] ‘Experimental studies on bubble pump operated diffusion absorption machine based on  
194 light hydrocarbons for solar cooling’. N Ben Ezzine , R Garma , M Bourouis , A Bellagi . *Ren. Energy* 2010.  
195 35 (2) p. .
- 196 [Ishii and Ktwo ()] ‘fluid model and hydrodynamic constitutive relations’. M Ishii , Mishima Ktwo . *Nucl Eng*  
197 *Design* 1998. 82 p. .
- 198 [Kh et al. ()] Hidouri Kh , A Benhmiden , R Benslama , S Gabsi . *Effects of SSD and SSDHP on convective heat*  
199 *transfer coefficient and yields*, 2009. 249 p. .
- 200 [Aman et al. (2016)] ‘Modelling and Analysis of Bubble Pump Parameters for Vapor Absorption Refrigeration  
201 Systems’. Julia Aman , S-K David , Paul Ting , Henshaw . *ASHRAE Annual Conference*, (St. Louis, MO  
202 USA) June (2016).
- 203 [Benhmidene et al. ()] ‘Modelling of Boiling Two-phase Flow in the Bubble Pump of Diffusion-Absorption  
204 Refrigeration Cycles’. A Benhmidene , B Chaouachi , S Gabsi , M Bourouis . *Chem. Eng. Commu* 2015.  
205 202 (1) p. .
- 206 [Benhmidene et al. ()] *Modelling of the heat flux received by a bubble pump of absorption-diffusion refrigeration*  
207 *cycles*, A Benhmidene , B Chaouachi , S Gabsi , M Bourouis . 2011. *Heat Mass Transfer*. 47 p. .
- 208 [Vicatos and Bennett ()] ‘Multiple lift tube pumps boost refrigeration capacity in absorption plants’. G Vicatos ,  
209 A Bennett . *J. Energy S. Africa* 2007. 18 p. .
- 210 [Garma et al. ()] ‘Numerical investigations of the heating distribution effect on the boiling flow in the bubble  
211 pumps’. R Garma , Y Stiriba , M Bourouis , A Bellagi . *Int. J. Hydrogen Energy* 2014. 39 p. .
- 212 [Benhmidene et al. ()] ‘Numerical prediction of flow patterns in the bubble pump’. A B Benhmidene , M  
213 Chaouachi , S Bourouis , Gabsi . *J. Flui Eng. ASME* 2011. 133 (3) p. 31302. (8 pages)
- 214 [Dammak et al. ()] ‘Optimization of the geometrical parameters of a solar bubble pump for absorption diffusion  
215 cooling systems’. N Dammak , B Chaouachi , S Gabsi , M Bourouis . *Am. J. Eng. Appl. Sci* 2010. 3 p. .
- 216 [Gurevich et al. ()] ‘Performance of a set of parallel bubble pumps operating with a binary solution of R134a-  
217 DMAC’. B Gurevich , M Jelinek , A Levy , I Borde . *App. Ther. Eng* 2015. 75 p. .
- 218 [Faisal ()] *Performance Study of LiBr-Water Pumpless Absorption Refrigeration System*, S Faisal . 2012. Basrah  
219 , Iraq; PhD Dissertation. University of Basah
- 220 [Shihab and Morad ()] A W.S Shihab , A M Morad . *Experimental Investigation of Water Vapor-Bubble Pump*  
221 *Characteristics and its Mathematical Model Reconstruction*, 2012. 30.

## 8 CONCLUSION

---

- 222 [Jakob et al. ()] ‘Simulation and experimental investigation into diffusion absorption cooling machines for  
223 airconditioning application’. U Jakob , U Eicker , D Schneider , A H Taki , M J Cook . *Appl. Therm.*  
224 *Eng* 2008. 28 p. .
- 225 [Jakob et al. ()] ‘Simulation and experimental investigation into diffusion absorption cooling machines for  
226 airconditioning applications’. U Jakob , U Eicker , D Schneider , M J Cook , A H Taki . *App. Ther. Engineering*  
227 2008. 28 p. .
- 228 [Pfaff et al. ()] ‘Studies on bubble pump for a water-lithium bromide vapor absorption refrigeration’. M Pfaff ,  
229 R Saravanan , M P Maiya , M Srinivasa . *Int J Refrigeration* 1998. 21 p. .
- 230 [Zohar et al. ()] ‘The influence of diffusion absorption refrigerant cycle configuration on the performance’. A  
231 Zohar , M Jelinek , A Levy , I Borde . *Appl. Therm. Eng* 2007. 27 p. .
- 232 [Chisholm ()] *Two-Phase Flow in Pipelines and Heat Exchangers*, D Chisholm . 1983. New York: Longman Inc.